Experimental investigation of the effect of temperature on the first desorption isotherm of concrete

Stéphane Poyet

Experimental investigation of the effect of temperature on the first desorption isotherm of concrete

Stéphane POYET

CEA Saclay, DEN/DANS/DPC/SCCME/LECBA, B158, 91191 Gif sur Yvette Cedex, France

1. Abstract

In the framework of the radioactive waste management in France, interim storage concrete structures should be submitted to temperature up to 80°C and subsequent desiccation. The impact of temperature on the sorption properties of concretes has been poorly studied and results are scarce. An experimental campaign was thus carried out to characterize the first desorption isotherms of a modern concrete at 30°C and 80°C. The results show a significant influence of the temperature increase that will have to be accounted for the durability assessment of the long-term interim storage concrete structures. Investigating the causes of these modifications, it appeared that desorption induced by temperature might be the principal mechanism rather than microstructure alteration and water properties evolution.

2. Introduction

In the framework of radioactive waste management, the concrete structures for radioactive waste management are expected to undergo significant heating due to the waste thermal power. In the French concept of subsurface structures, the cooling is likely to be achieved using natural convection with air taken from outside. Doing so, the concrete temperature is expected to reach (but not to exceed) 80°C in normal conditions and the concrete structure is expected to undergo severe drying (due to the temperature increase of the ambient air) [1; 2]. The durability assessment of these structures over 300 years thus requires the accurate knowledge of the sorption properties of concretes at such unusual temperature levels with particular interest in desorption (corresponding to the drying process).

The influence of temperature on the sorption isotherms has been poorly studied and experimental results are scarce in the scientific literature. Among these studies Daïan has experimentally determined the adsorption isotherms of a water-cured mortar at four different temperatures: 20, 35, 45 and 55℃ [3; 4]. The samples have been initially dried at 80℃ and then exposed to different increasing RH for the four temperatures. The curves thus obtained are reproduced on Fig. 1 (according to the results published in [4]). The temperature influence can be summarised as follows: the higher the temperature, the less the amount of water adsorbed. Nevertheless, the offset between the curves obtained at 20℃ and 55℃ was found to be low.

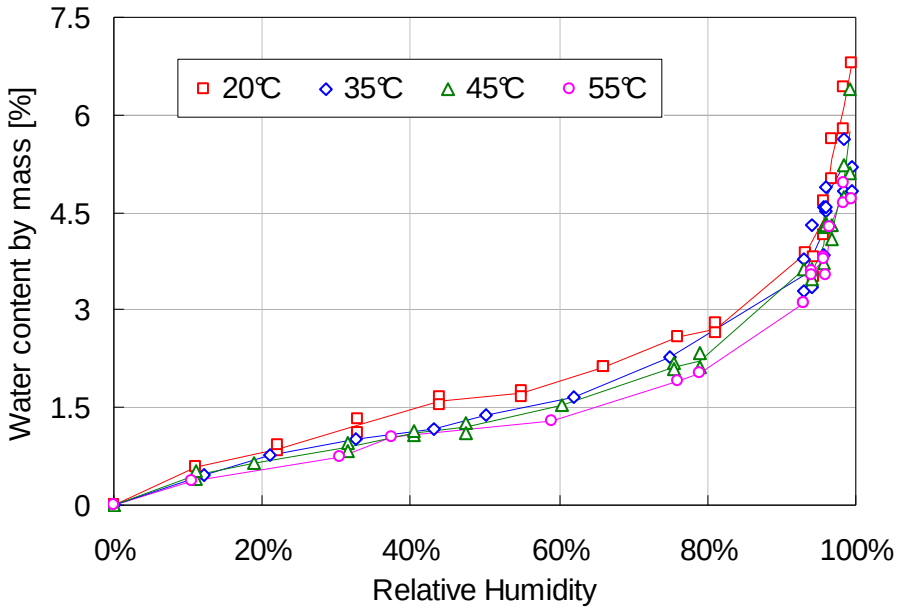

Fig. 1. Adsorption curves for a mortar between 20℃ and 55℃ after Daïan [4].

This observation is in good agreement with the experiments of Radjy et al. [5] who characterised the first adsorption branch of two mature (about two years old) steam-cured at early-age (at nearly 100℃) hardened cement pastes with water-to-cement ratio (W/C ratio) equal to 0.35 and 0.45 respectively for temperatures between 0℃ and 60℃. The results have shown a very limited dependence of the isotherms to temperature in this range. In the same way, the first desorption isotherm of a mature (kept one year under water) hardened cement paste cured at ambient temperature with a W/C ratio equal to 0.50 was characterised

for temperatures between 0℃ and 40℃. As mentioned before, the resulting desorption isotherms showed hardly any dependence on the temperature used.

In a recent attempt to develop a model capable of predicting the behaviour of concrete in any arbitrary environment Ishida et al. [6] have characterised the sorption isotherms (the first adsorption and the first desorption branches) of an 80-day water-cured hardened cement paste (W/C ratio equal to 0.50) for 20℃, 40℃ and 60℃. The results obtained for the first adsorption have shown little differences between the curves for the three temperatures. However, the results of the first desorption appeared to be much different: the first desorption isotherm was greatly modified by the temperature increase. The decrease of the amount of water adsorbed at higher temperatures was more pronounced than that obtained for adsorption. Moreover the shape of the isotherms was also modified by the temperature increase.

These facts have already been pointed at by Hundt & Kantelberg [7] who characterised the first desorption isotherm of different cementitious materials for temperatures ranging from 20℃ to 70℃. The results obtained with a 3.6 year old mortar (W/C ratio equal to 0.50) are reproduced on Fig. 2 (according to the data published in [7]). As mentioned before the higher the temperature, the less the amount of water adsorbed at equilibrium. One can see on Fig. 2 that the 20℃ desorption isotherm was nearly a straight line. This pattern was greatly modified when working at higher temperatures: see for instance the linear part between 20% and 50% with a decreasing slope related to the temperature increase and the pronounced upwards deviation for high RH. In addition, one can note the significant decrease of the amount of water adsorbed at saturation as a function of temperature: the higher the temperature, the lesser the amount of water at saturation. Hardened cement pastes with varying W/C (between 0.40 and 0.55) and concretes with various preliminary treatments were also tested by Hundt & Kantelberg [7], all the results obtained in this study (various cementitious materials with various curing methods) confirm all these observations.

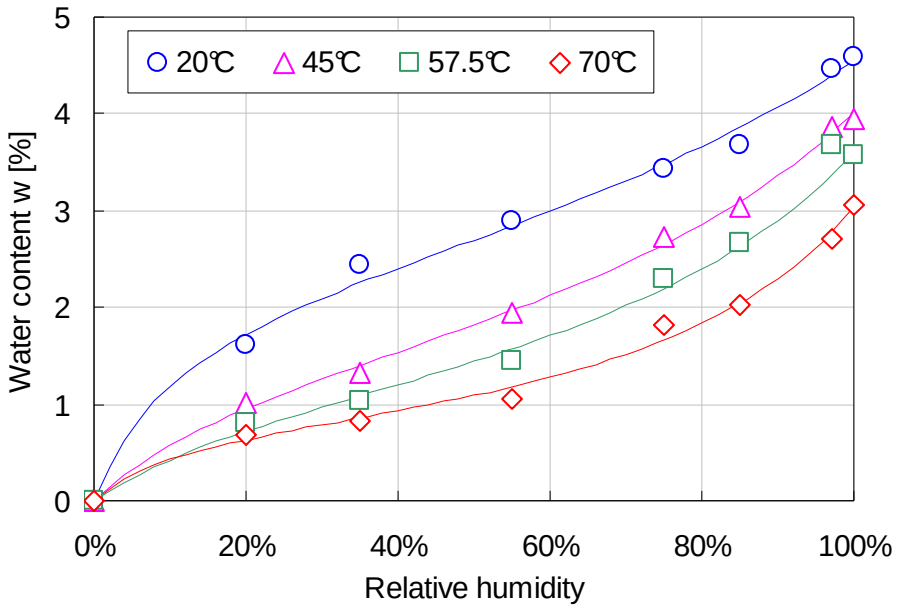

Fig. 2. First desorption isotherms for a mature mortar for four temperatures ranging from 20℃ to 70℃ according to Hundt & Kantelberg [7].

An experimental campaign was then undertaken to highlight the influence of temperature and gather experimental data for further numerical approaches and durability assessment of interim storage concrete structures. The first desorption isotherm of a modern high-performance concrete was characterised at 30℃ and 80℃. The temperature dependence of cementitious materials sorption properties is generally related to the coarsening of the pore structure (ettringite dissolution and C-S-H alteration) together with the evolution of water properties [8-11]. In this study, the examination of the results obtained indicates that another phenomenon may be at work and suggests that the microstructure alteration and the water properties evolution may have negligible effects.

3. Experimental programme

3.1. Material tested

The material used for the experiments was a modern high-performance concrete, the formulation is reported on Tab. 1. It is based on CEM I cement. The water-to-cement ratio (by weight) is equal to 0.43. This formulation was used because it is one of those which are

studied in the framework of radioactive waste management by the French agency for radioactive waste management (Andra).

Tab. 1. Concrete formulation

Component	Nature	Origin	Qty	Unit
Cement	CEM I 52.5	Lafarge Val d'Azergues, France	400	kg/m^3
Sand	Calcareous [0-5]	Boulonnais quarry, France	858	kg/m^3
Gravel	Calcareous [5-12.5]	Boulonnais quarry, France	945	kg/m^3
Water	-	-	172	L/m^3
Superplasticizer	Glenium 27	BASF	10	kg/m^3

The main properties of the concrete have been determined experimentally on samples taken out of the same batch and cured more than one year under water at 20℃. The values obtained are reported on Tab. 2. All the characterization tests were performed on saturated samples at 20℃ (except for the gas permeability measurements and water porosity which implied complete drying at 60℃) and after thermal treatment at 80℃ (until constant mass was achieved, residual properties after cooling). The intrinsic permeability to gas (nitrogen) was estimated using the Klinkenberg approach [12].

Tab. 2. Main concrete properties, all given data are at least the mean of three values

Concrete properties	20℃	80℃	Unit
Tensile splitting strength (Brazilian test)	5.80	4.95	MPa
Compressive strength	89.7	79.5	MPa
Elastic modulus	49.2	41.7	GPa
Poisson's ratio	0.18	0.17	-
Water porosity	11.3	12.0	%
Intrinsic permeability (nitrogen)	$2.0 \cdot 10^{-17}$	$4.2 \cdot 10^{-17}$	m^2
Klinkenberg coefficient	0.13	0.06	MPa
Heat conductivity	2.49	2.09	W/mK

The porosity to water at 30℃ and 80℃ was estimated using the mass loss obtained using silica gel (RH~3%). It was also estimated using two other usual experimental protocols: drying at 60℃ with silica gel and drying at 105℃. All the results are presented in Tab. 3. The concrete saturated density was calculated using hydrostatic weighing, the mean value was found to be equal to 2.48.

Tab. 3. Porosity to water according to the experimental protocol.

Protocol	30℃ (silica gel)	60℃ (silica gel)	80℃ (silica gel)	105℃ (no silica gel)
Porosity to water	10.7%	11.3%	12.0%	12.3%

3.2. Technique used

The concrete first desorption isotherm was determined at 30℃ and 80℃. The desiccator method using saturated salt solutions was chosen for its simplicity and its reliability. This is a standalone system which minimises human interventions and is recommended by the European Committee for Standardization [13]. The different RHs which were used are given in Tab. 4. For RH=100% deionised water was used (without any salt) and for RH=3% silica gel was used (without water). The saturated salt solutions were prepared according to international recommendations [13; 14] and the resulting RHs were verified before use.

Tab. 4. RH investigated and corresponding saturated salt solutions.

Salt used	Formula	RH obtained at	
		30℃	80℃
Deionised water	H_2O	100%	100%
Potassium sulphate	K_2SO_4	96%	95%
Sodium sulphate	Na_2SO_4 10 H_2O	-	90%
Potassium nitrate	KNO_3	90%	-
Potassium chloride	KCl	85%	-
Sodium chloride	NaCl	75%	74%
Sodium nitrate	$NaNO_3$	-	65%
Ammonium nitrate	NH_4NO_3	63%	-
Sodium bromide	NaBr	55%	51%
Potassium carbonate	K_2CO_3	-	42%
Magnesium chloride	$MgCl_2$ 6 H_2O	33%	26%
Lithium chloride	LiCl	12%	10%
Silica gel	SiO_2	3%	3%

3.3. Sample preparation

Characterization of the sorption isotherm using the gravimetric method requires long-term experiments due to the samples dimensions and water transfer properties of the materials tested. In order to reduce the experiment duration the samples used usually have small dimensions: thin slices [15-17], powders [18-20], crushed or sawn small specimens (up to one centimetre max) [4; 6; 20-22]. One can note that such sample shape and dimensions greatly differ from a concrete Representative Volume Element (RVE). In addition, if the sample preparation has an effect on the experiments (for instance superficial microcracking

120 or carbonation) then this effect may concern a great part of the sample volume because of its
121 thinness.
122 In this study an attempt was made to use massive samples as close as possible to a RVE.
123 Hence “massive” cylindrical specimens with diameter and height equal to 40 mm were used.
124 One could note that this dimension is far from the minimum 100 mm recommended in the
125 European standard EN 123901 [23], nevertheless this value appeared as the best
126 compromise between the duration of the experiments and the representativeness of the
127 samples (the weight of the resulting samples was about 120 grams.)
128 The samples were cored from 11 cm x 22 cm specimens cured under water (with added
129 lime) at 20°C at least one year after casting. All the samples were taken from the same batch
130 (the one used for the characterisation whose results are presented in Tab. 2). No
131 preventative measure was taken to prevent carbonation since it is expected to affect only a
132 small zone at the surface of the samples that is to say a negligible volume when compared to
133 the total volume of the samples.

134 *3.4. Dry and saturated states*

135 The reference dry state is essential for the correct evaluation of the sorption curves. It is
136 generally estimated using oven-drying. This treatment is known to be too aggressive for
137 cement-based materials (microcracking and modification of pore network) and alternate
138 techniques do exist (isothermal drying using hydrophilic compounds, solvent exchange, D- or
139 P-drying…) [24-29]. Yet as far as only desorption is concerned (no preliminary drying and no
140 further resaturation) oven-drying at 105°C was chosen as the reference dry state.
141 The initial saturated state was achieved using the one-year cure under water (with lime to
142 prevent carbonation). No other specific procedure was used (for instance resaturation using
143 vacuum).

3.5. Experimental protocol

The best method for the characterisation of the first desorption isotherm consists in submitting a unique set of initially saturated samples to decreasing RH steps and waiting for equilibrium for each step [5; 7; 20; 30; 31]. This method was inappropriate for this study given that the time needed to reach equilibrium was expected to be too long due to the massive samples used. It was then decided to use different set of samples to be submitted to a unique RH. The number of sample set for each temperature (30°C and 80°C) was equal to the number of salt solutions (10 sets for each temperature including deionised water and silica gel, see Tab. 4). This method allowed the simultaneous determination of each point of the curve and a corresponding estimated reduction of the experiments time by a factor 10. It was however expected to induce some variability since different specimens were to be used.

Fig. 3. View of the 40 mm x 40 mm samples and the climatic boxes containing the saturated salt solutions. Note the opening at the top of the containers which allows inserting a probe for verification of both temperature and RH.

The 40 mm x 40 mm cylinder samples were weighed in air and under water before the beginning of the experiments and their volume and saturated density were computed (weighing was carried out using a 1 mg accurate device). They were then put in hermetic

161 containers by groups of three above the saturated salt solutions and the containers were
162 kept in two different ovens regulating the temperature to 30℃ and 80℃. A view of the
163 40 mm x 40 mm samples and of the hermetic containers is presented in Fig. 3. The
164 containers were opened periodically to measure the mass of the samples. The latter were left
165 as long as possible in the containers in order to get as close as possible to equilibrium.

166 4. Experimental results

167 *4.1. Mass variation and water transfer properties*

168 On the basis of the periodic mass measurements, the mean relative mass variation *(Δm/m)*
169 of the samples for each temperature and RH could be computed following the classical
170 relation:

171 $$\left(\frac{\Delta m}{m}\right)(t) = \frac{m(t) - m_0}{m_0}, \qquad (1)$$

172 where m_0 and $m(t)$ are the initial sample mass (saturated) and the mass for the time t. The
173 results are presented in Fig. 4 and Fig. 5 for 30℃ and 80℃ respectively.

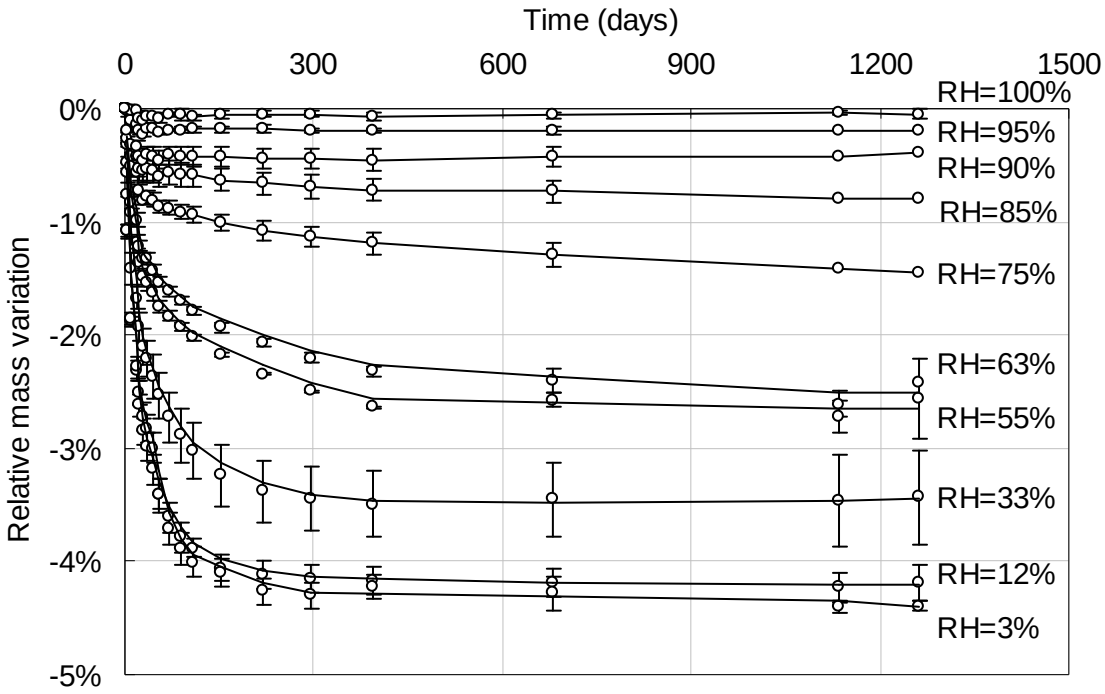

174

175 Fig. 4. Mass variation of the samples kept at 30℃ (each value is the average value obtained

176 using three samples, the error bar stands for the standard deviation).

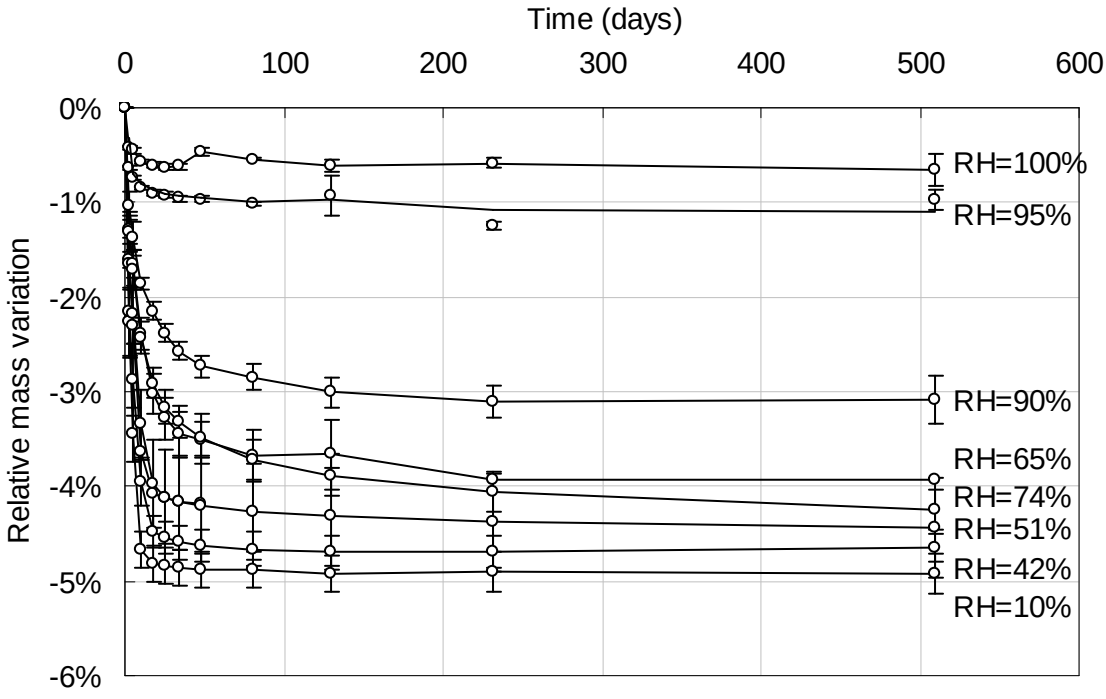

177

178 Fig. 5. Mass variation of the samples kept at 80℃ (each value is the average value obtained

179 using three samples, the error bar stands for the standard deviation).

The desorption experiments spanned over 1200 days and 500 days for 30℃ and 80℃ respectively. Such experiment durations (qualitatively) appear to be sufficient to reach equilibrium at 80℃ but not at 30℃ for which the s amples kept between 55% and 85% still present mass variation after 1200 days. Nevertheless, the amount of water in excess (with respect to the equilibrium to be reached) is expected to be low and the corresponding error negligible. One can note that for each temperature the patterns are similar: the mass loss kinetics is maximal in the early days, it is then continuously reduced as far as the drying proceeds and the equilibrium is approached. In addition, the lower the RH the higher the mass loss. The main differences between the results for both temperatures lie in the mass loss kinetics and in the value reached at equilibrium (the last point will be discussed in the next chapter).

When examining Fig. 4 and Fig. 5 it is obvious that the time needed to reach the equilibrium at 80℃ is much lower than the one needed at 30℃. For instance, the time needed to reach 90% of the mass loss is about one month at 80℃; it is extended to more than one year at 30℃. This point has already been studied by severa l authors who showed the drying acceleration and the increase of the water transfer properties with temperature [32-36].

4.2. First desorption isotherms

In order to determine the first desorption isotherms at 30℃ and 80℃, the amount of water retained according to the RH was expressed using the mass water content *w*:

$$w(T,RH) = \frac{m_w(T,RH)}{m_s}, \quad (2)$$

where m_w and m_s are the mass of adsorbed water and the mass of the dry material respectively. It was computed using the experimental mass variations ($\Delta m/m$):

$$w(T,RH) = \frac{d_{sat}}{d_{sat}-\phi}\left[\left(\frac{\Delta m}{m}\right)(T,RH) + \frac{\phi}{d_{sat}}\right], \quad (3)$$

where d_{sat} and ϕ are the saturated initial density and the porosity respectively. The results are presented in Fig. 6, the reference dry state was fixed using oven drying at 105℃; that is to say the value of the porosity ϕ needed in eq. (3) is equal to 12.3%.

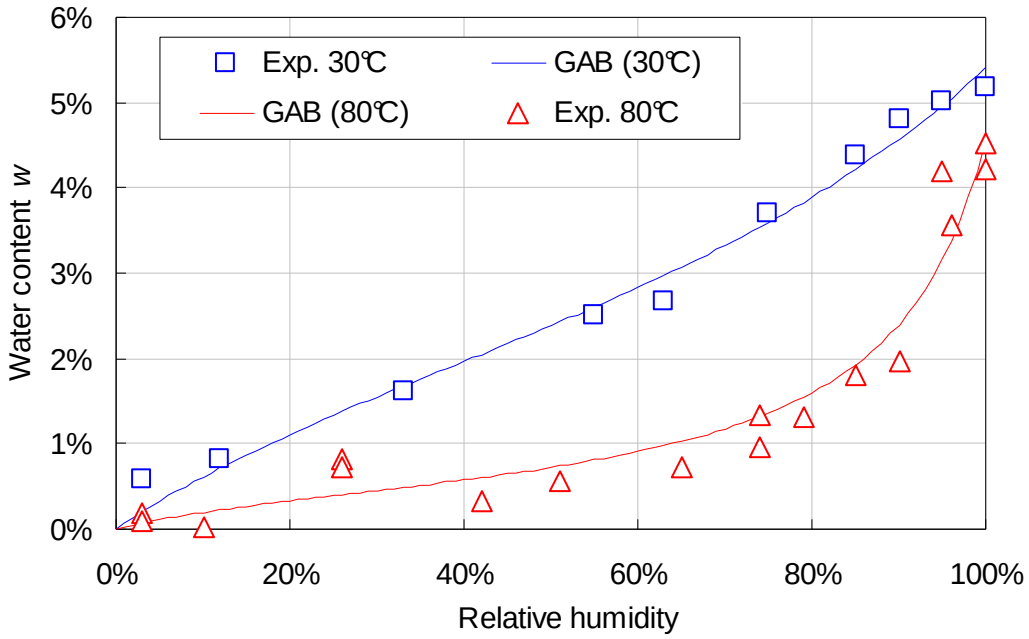

Fig. 6. First desorption isotherms at 30℃ and 80℃.

The symbols stand for the experimental results derived from the experiments whereas the solid lines stand for a curve-fitting using the GAB model [37-39]. The GAB model is a three-parameter which is an evolved version of the BET model (with a supplementary parameter k), it can be written as follows:

$$w(h) = \frac{Ckw_m h}{(1-kh)[1+(C-1)kh]}, \quad (4)$$

where C, k and w_m are the three parameters of the GAB model and h is the relative humidity. The GAB model is used here because it is based on physical phenomena (which yield a correct isotherm shape), it was shown that it can be used almost over the whole RH range and offers the best fit among various adsorption models [37; 40-43]. Moreover this model is widely used in various fields and it has already proven its suitability for cementitious materials [44-46]. The values of the three parameters of the GAB model are reported in Tab. 5.

220 Tab. 5. Data for the fitting of the GAB model at 30℃ and 80℃.

Temperature	C [-]	k [-]	w_m [kg/kg]
30℃	4.690	0.592	2.534%
80℃	6.010	0.897	0.480%

221

222 Looking at Fig. 6, one can easily notice that temperature has a tremendous impact on the
223 first desorption isotherm: at 30℃ the curve can almost be described by a straight line from
224 the origin up to the saturation point ($w \approx 5.4\%$) whereas at 80℃ high non-linearity appears.
225 In addition to the alteration of the curve morphology, one can note that for a given RH the
226 water content at equilibrium is always reduced at 80℃ (when compared to the values
227 obtained at 30℃). This effect even appears for RH= 100%: an initially saturated sample
228 whose temperature is suddenly increased up to 80℃ undergoes a significant mass loss:
229 from 5.4% to 4.6%. The reduction of the water content at equilibrium is not constant over the
230 whole RH range; for instance for RH=100% the difference in the water content is about 0.8%
231 (absolute value) whereas it is about 2.3% for RH=80%. This effect can be, for instance,
232 quantified using the water content ratio (by mass) r_w:

233 $$r_w(RH,T) = \frac{w(T,RH)}{w(30°C,RH)}. \quad (5)$$

234 Fig. 7 presents the evolution of the water content (by mass) r_w as a function of RH for the
235 experiments presented in this study. Data derived from the work of Hundt & Kantelberg [7]
236 are also presented; in this case the two temperatures were 20℃ and 70℃, and different
237 cementitious materials were used (hardened cement pastes with different W/C, mortar and
238 concrete with different cures or preconditioning methods). Despite these differences, one can
239 note that the results obtained in this study are in good agreement with the results of Hundt &
240 Kantelberg. The water content ratio appears not to be constant over the full RH range: the
241 general shape of the curve is parabolic and thus presents a minimum value of about 0.3
242 which is roughly located at RH=35%. The maximal value of the ratio r_w=0.85 is reached at
243 saturation (for RH=100%). This fact is very important, because it means that the saturation
244 state is not constant versus temperature. It implies that a saturated concrete becomes

oversaturated when the temperature increases. As a consequence the concrete is out of equilibrium and water is released and evacuated into the environment: this phenomenon can clearly be seen on Fig. 5 on which the mass loss of saturated samples kept at RH=100% and 80℃ can be seen whereas saturated samples kept at 30℃ and RH=100% do not exhibit such behaviour (Fig. 4).

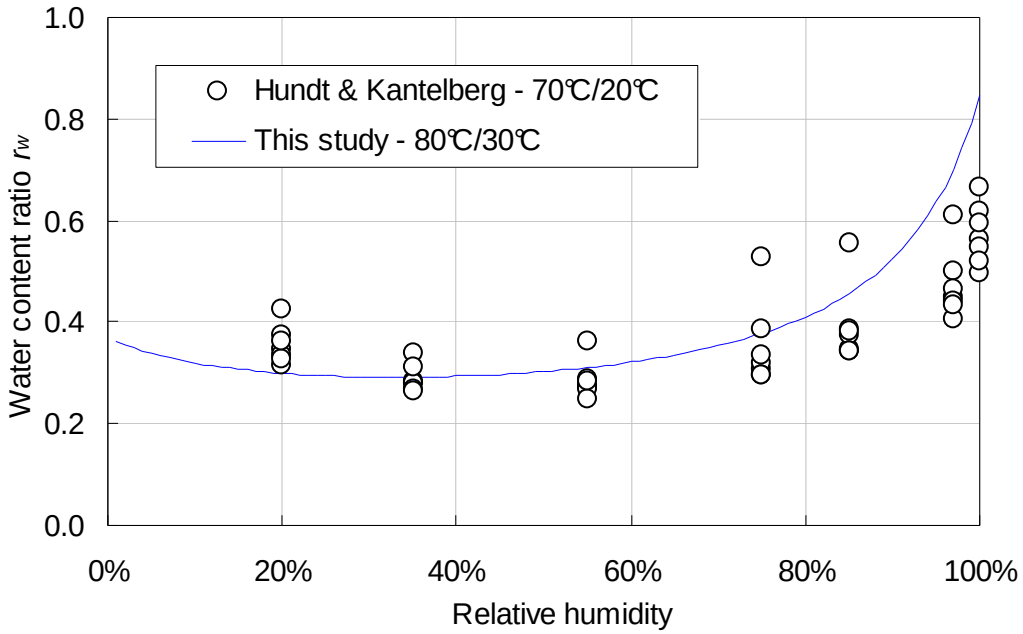

Fig. 7. Evolution of the water content ratio r_w as a function of RH.

4.3. Pore structure investigation

In order to quantify the influence of temperature on the first desorption isotherm, the specific surface area S_{BET} was estimated using the BET model [47]:

$$w = \frac{C w_m h}{(1-h)[1+(C-1)h]}, \quad (6)$$

where C and w_m are two positive parameters of the BET model. w_m is the mass of water (for one gram of dried material) needed to complete a monomolecular adsorbed layer, its value is used to compute the specific surface area S_{BET}. According to the recommendations of the IUPAC [48] the BET parameters were not estimated using the experimental data from the full RH range. However, due to the lack of experimental data in the low RH (typically between 5% and 30%) the fitting interval was extended up to RH=50%. In so doing, it was accepted

that this would not yield an accurate value of the specific surface, rather only a rough estimate. The fitted parameters are reported in Tab. 6.

Tab. 6. Data for the fitting of the BET model.

Temperature	30℃	80℃
C [-]	20.8	22.0
w_m [m^3/kg]	1.16%	0.35%
S_{BET} [m²/g]	41	13

The specific surface area S_{BET} was estimated using [49]:

$$S_{BET}(T) = w_m(T)\frac{A_w}{\rho_w V_w}(T)N_A\,, \tag{7}$$

where V_w and N_A are the molar volume of water ($0.1808\cdot10^{-4}$ m^3/mol and $0.1853\cdot10^{-4}$ m^3/mol at 30℃ and 80℃ respectively) and Avogadro's numbe r ($N_A = 6.02\cdot10^{23}$) and A_w is the area occupied by a single water molecule on the surface of the sample. The latter was estimated using the equation [50; 51]:

$$A_w(T) = 1.091\left[\frac{M_w}{N_A\rho_w(T)}\right]^{\frac{2}{3}}, \tag{8}$$

where M_w is the molar mass of water ($18\cdot10^{-3}$ kg/mol). The resulting coverage areas for one molecule of water A_w are 10.538 Å² and 10.712 Å² at 30℃ and 80℃ respectively. These values are very close to 10.508 Å² used by Baroghel-Bouny (for 23℃). Many different values were used to calculate S_{BET} in the literature (ranging from 10.5 Å² to 12.5 Å²) leading to discrepancies in the specific surface area estimations and major difficulties of comparison between all the published results [46; 52]. All the data used for the estimation (V_m and A_w in particular) are however reported here which allows to estimate S_{BET} using different data.

The specific surface area obtained at 30℃: the res ult is S_{BET}(30℃) = 41 m²/g. This value is consistent with the data published (using water vapour): roughly ranging from 20 to 200 m²/g according to the cementitious material tested and the technique used [15; 22; 29; 52-57]. The value of the specific surface area S_{BET} is divided by 3 when measured at 80℃ and falls do wn to S_{BET}(80℃) = 13 m²/g (Tab. 6). These data are comparabl e to the results obtained by Bray & Sellevold [58] and Radjy & Richards [19] who showed that a temperature increase

between ambient temperature and 90℃ or 100℃ resul ted in a decrease of the BET monolayer parameter V_m estimated using water desorption experiments (and thus the specific surface area S_{BET}).

In the same time, Mercury intrusion porosimetry (MIP) experiments were performed to highlight the influence of the desorption temperature on pore size distribution. The samples used for the desorption experiments at 30℃ and 80° C and kept at RH=3% were used. They were crushed into small parts (several millimetres), frozen by immersion into liquid nitrogen, let to dry under vacuum for seven days and then tested at ambient temperature. The results are presented on Fig. 8. One can see that for the two desorption temperatures a bi-modal pore size distribution is obtained corresponding to C-S-H nanoporosity (around 3 nm) and capillary porosity (around 100 nm). For desorption at 30℃, the access diameter for capillary porosity is about 70 nm. Desorption at 80℃ appears to slightly shift it towards larger diameters (110 nm) as it was already shown [25; 59]. The variability observed in the intruded volume was not thought to be significant and assumed to be related to the presence of sand and aggregates in the samples together with hardened cement paste.

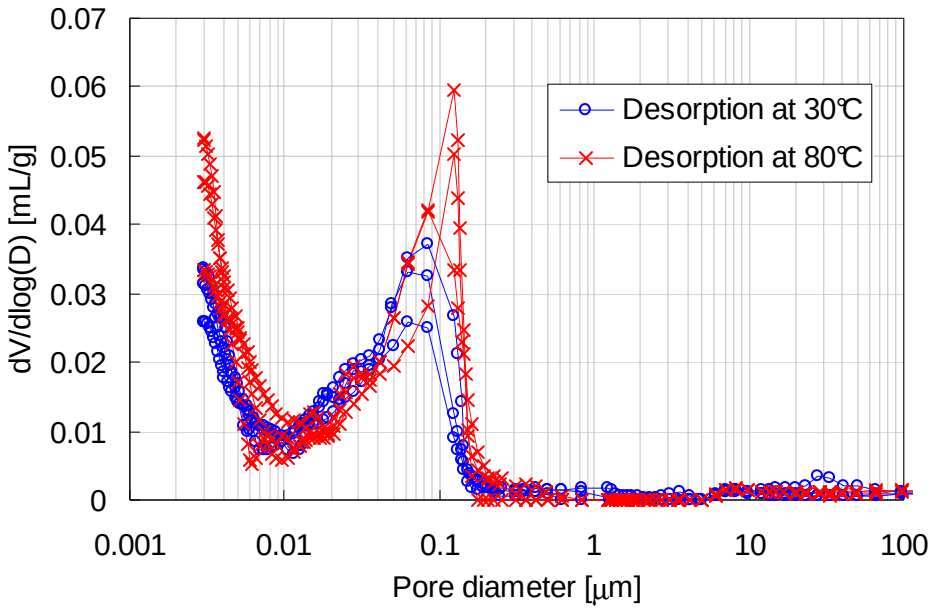

Fig. 8. Pore size distributions obtained by MIP after desorption at 30℃ and 80℃.

The specific surface areas estimated using MIP were quite different from the ones derived from desorption. A value of about 10 m^2/g after desorption at 30℃ was obtained; the same value (12 m^2/g) was obtained for desorption at 80℃ in contradiction with desorption results.

5. Discussion

The (slight) increase of the capillary porosity average access diameter between 30℃ and 80℃ observed using MIP as well as the decrease of the specific surface area are consistent with the desorption isotherm modification: the coarser the pore size, the greater the upward deviation (see for instance [22] for compacted cement pastes; [56; 60] for hardened cement pastes with variable water-to-cement ratio and [61-65] for compacted powders.) Yet one must note that the porosity increase (between 30℃ and 80℃, Tab. 3) is not compatible with the fall of the water content at saturation (it is expected to induce a water uptake at saturation leading to mass gain.) The latter may be explained by the decrease of water density when temperature is increased.

However these two phenomena are believed by the author to have a small impact on the isotherms: the decrease of water density (at least between 20℃ and 80℃) as well as the coarsening of the pore structure as observed using MIP remain very limited. In the author's mind, these two phenomena cannot explain the important modifications of the desorption isotherm observed between 30℃ and 80℃. Moreover t he difference of specific surface areas obtained using the 80℃ isotherm and MIP led the author think that another phenomenon directly linked to temperature might be at work.

Such a phenomenon can be described as follows: adsorption is an exothermic process [66; 67] and according to the principle of Le Chatelier and the rule of Van't Hoff: the effect of a change in temperature on a system at equilibrium is to shift the equilibrium in the direction that acts to counteract and nullify the temperature change. This means increasing temperature hinders adsorption and promotes desorption; as a consequence a lesser number of molecules can be adsorbed. This phenomenon is very well-known in adsorption science. Many studies can be found in the literature which show the impact of temperature

329 on sorption isotherms for different adsorbents and adsorbates [50; 68-73], the results always
330 show the same modifications of the sorption isotherms as described in this paper.
331 Furthermore in adsorption technology, the temperature increase and the heat transfers
332 induced by the heat of adsorption are accounted for the design of the adsorbent beds (to
333 avoid the performance reduction due to temperature increase) and thermal treatments at
334 elevated temperature are usually used as a method to regenerate adsorbents (this method is
335 also know as “temperature swing adsorption”) [73; 74].
336 This effect can be described using the Clausius-Clapeyron equation which permits the
337 evaluation of the heat involved in a change of phase for a system in equilibrium, in the case
338 of adsorption it can written under the form [66]:

339 $$Q_{st}(w) = -R\left[\frac{\partial \ln(p_v)}{\partial\left(1/T\right)}\right]_w, \quad (9)$$

340 where Q_{st} is the isosteric heat of adsorption [J/mol], T and R are the absolute temperature [K]
341 and the universal gas constant (R = 8.3145 J/mol/K) and p_v is the water vapour pressure [Pa]
342 at equilibrium with the adsorbed quantity w respectively. In our case the heat of adsorption
343 could be estimated using the two isotherms obtained at 30℃ and 80℃ using the integrated
344 form of eq. (9):

345 $$Q_{st}(w) = -R\frac{T_1 T_2}{T_1 - T_2}\ln\left[\frac{p_v(T_1,w)}{p_v(T_2,w)}\right], \quad (10)$$

346 where $p_{v1}(w)$ and $p_{v2}(w)$ are the vapour pressures at equilibrium with the water content w for
347 the temperatures T_1 and T_2 respectively. In so doing, it was implicitly assumed that the pore
348 size distribution and the water properties remain constant over the whole temperature range.
349 Fig. 9 presents the resulting evolution of the isosteric heat of desorption as a function of
350 water content. One can see that the isosteric heat of desorption is a decreasing function of
351 water content: the high value observed for low water contents is representative of strong
352 bonding between the adsorbed water molecules and the cementitious substrate whereas the
353 decrease can be related to the drop of the influence of the substrate with the increase of the
354 distance between adsorbed water molecules and substrate. The value reached at high water

355 contents is equal to the average enthalpy of condensation (42.7 kJ/mol between 30 and
356 80°C): it can be considered that there is no more influence of the substrate and water
357 molecules are bound the ones to the others (condensation).
358 For verification purpose, the isosteric heat of desorption obtained in this study was compared
359 to the one proposed by Powers & Brownyard [60]. They used the heat-of-solution method on
360 two hardened cement pastes. The method consists in dissolving paste samples in a
361 calorimeter and measuring the heat evolved. Repeated measurements on samples
362 contained different amounts of adsorbed water allowed them to evaluate the isosteric heat of
363 adsorption which can be written under the following form (in kJ/mol):

364 $$Q_{st}(w) = L + \frac{64.6}{(1.31 + w/w_m)^2}, \quad (11)$$

365 where L = 42.7 kJ/mol is the average condensation enthalpy of water within the range 30-
366 80°C. The comparison is presented on Fig. 9. One can see that except for low values of
367 w/w_m (below 0.2), there is a good agreement between the two curves. This fact is important
368 since Powers & Brownyard performed their experiments at constant (ambient) temperature.
369 This seems to indicate that the two phenomena initially identified to explain the influence of
370 temperature (coarsening of the pore structure and water properties evolution) might be
371 negligible in front of the desorption induced by temperature.

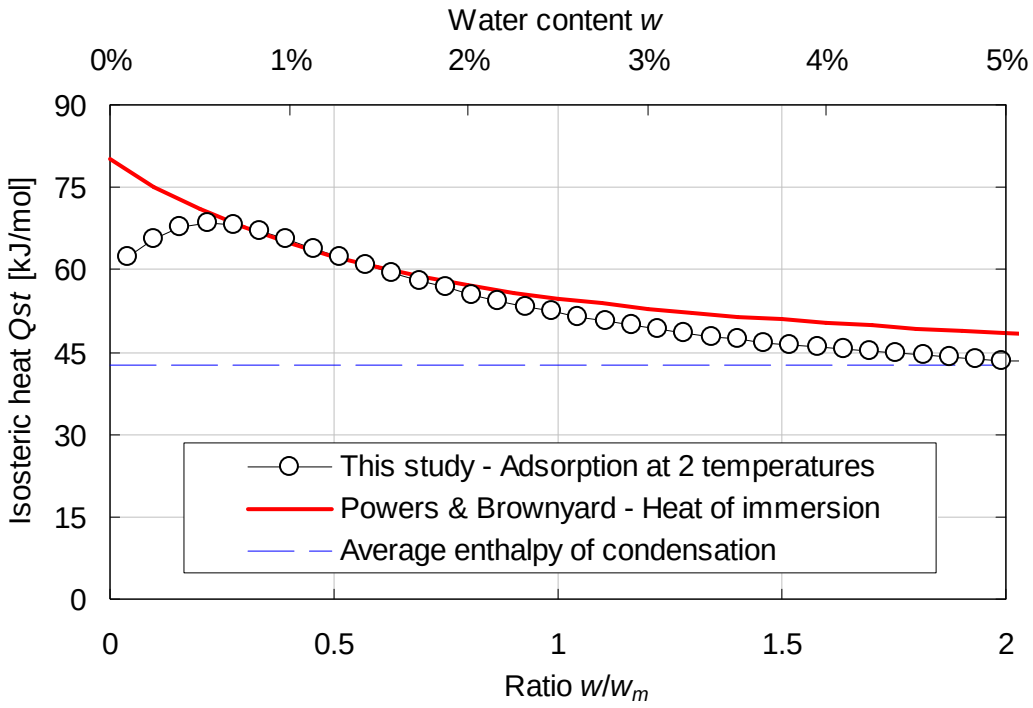

372

373 Fig. 9. Comparison between the isosteric heat of desorption obtained in this study (two
374 isotherms at two different temperatures and Clausius-Clapeyron) and the one proposed by
375 Powers & Brownyard using heat-of-solution tests (at ambient temperature).

376 Using Clausius-Clapeyron and the corresponding isosteric heat of desorption, it is possible to
377 estimate the water content ratio $r_w(RH,T)$ (as defined in eq. (5)) for any arbitrary temperature.
378 Fig. 10 presents the results obtained for temperatures ranging from 35℃ to 80℃. One can
379 see that the fall of water content increases with temperature and whatever the temperature,
380 the first desorption isotherm is expected to be modified: there is no threshold temperature.
381 Moreover, the change depends on the temperature level: for a small temperature increase
382 only the low-RH part of the isotherm is expected to be influenced whereas the isotherm is
383 expected to be modified over the whole RH range for higher temperatures.

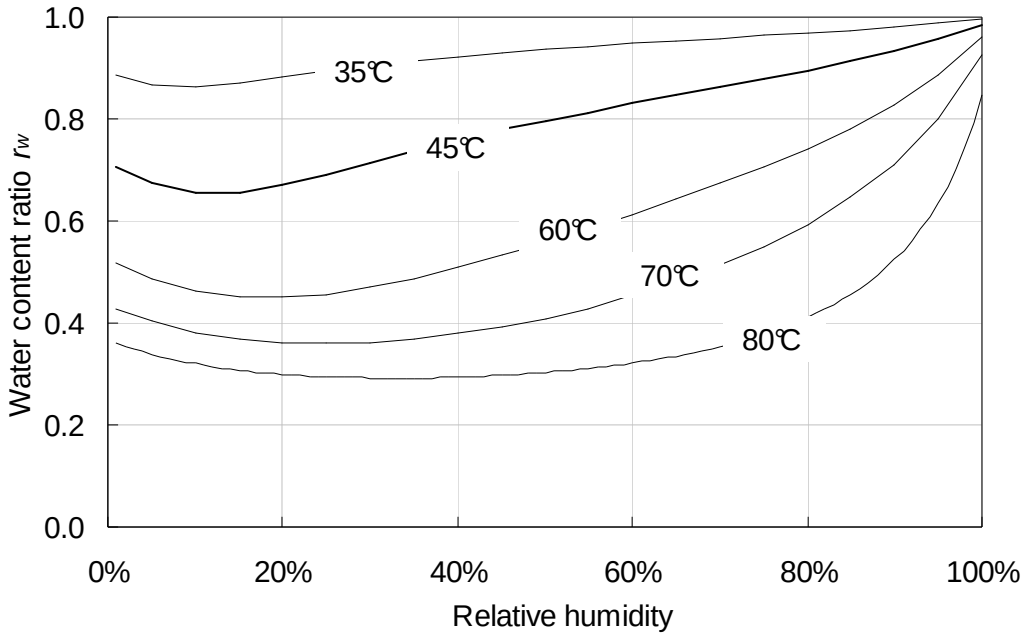

Fig. 10. Evolution of the ratio $r_w(RH,T)$ as a function of temperature and relative humidity.

6. Conclusion

In the framework of radioactive waste management and especially in the case of interim storage, concrete structures should be submitted to temperature up to 80℃ and subsequent drying. The durability assessment of such structures in such unusual conditions thus requires the knowledge of the first desorption isotherm at 80℃. An experimental campaign was thus undertaken to characterize the first desorption isotherms (at 30℃ and 80℃) of a French reference concrete for radioactive waste management. This was done using the desiccator method with massive samples. The results showed an important impact of temperature on the first desorption isotherm:

1. the general shape of the isotherm is modified and leads to more pronounced non-linearities;
2. the water content at equilibrium is drastically reduced at 80℃ over the whole RH range;
3. the water content at saturation at 80℃ is signi ficantly lower than at 30℃.

The examination of the results led the author to think that the coarsening of the pore structure and the evolution of water properties could not explain these important modifications and that another phenomenon was at work. The latter consists in desorption induced by temperature and can be described using Clausius-Clapeyron formula. Using the two isotherms acquired, it was possible to evaluate the isosteric heat of desorption and to compare it to the data obtained by Powers & Brownyard using a different method at constant temperature. The two of them are in good agreement. This seems to indicate that the temperature induced desorption is the predominant phenomenon in our experiments (for temperatures less than 80°C.)

7. Acknowledgements

This work was part of a project funded by Electricité de France (EdF) and the French agency for radioactive waste management (Andra). The author would like to thank Xavier Bourbon (Andra/DS) and Yann Le-Pape (EdF/DER) for their scientific support and also Guillaume Ranc who has initiated this study, Philippe Pétrini for his help in preparing and performing the experiments. Profitable discussions with Sébastien Charles and Christophe Gallé are gratefully acknowledged.

8. References

[1] H. Lagrave, Dossier de définition pour l'entreposage de longue durée des déchets HAVL et des combustibles usés (in french), CEA Internal Report DTEC/2005/10 (2005) 55p.

[2] H. Lagrave, Dossier de définition de l'entreposage de longue durée des déchets MAVL ou de catégorie B (in french), CEA Internal Report DTEC/2005/11 (2005) 63p.

[3] J.-F. Daïan, Processus de condensation et de transfert d'eau dans un matériau méso et macroporeux - Etude expérimentale du mortier de ciment (in french), Ph-D Thesis, Institut National Polytechnique de Grenoble (INPG), 1986, 319p.p.

[4] J.-F. Daïan, Condensation and isothermal water transfer in cement mortar, part I - pore size distribution, equilibrium, water condensation and imbibition, Transport in Porous Media 3(6) (1988) 563-589.

[5] F. Radjy, E.J. Sellevold, K.K. Hansen, Isosteric vapor pressure-temperature data for water sorption in hardened cement paste: enthalpy, entropy and sorption isotherms at different temperatures, Report BYG-DTU R057, Technical University of Denmark (DTU), Lyngby, Denmark, 2003, 58p.

[6] T. Ishida, K. Maekawa, T. Kishi, Enhanced modeling of moisture equilibrium and transport in cementitious materials under arbitrary temperature and relative humidity history, Cement and Concrete Research 37(4) (2007) 565-578.
[7] J. Hundt, H. Kantelberg, Sorptionsuntersuchungen an zemestein, zementmörtel und beton (in german), Deutscher Ausschuss für Stahlbeton Heft 297 (1978) 25-39.
[8] Z.P. Bažant, W. Thonguthai, Pore pressure and drying of concrete at high temperature, Journal of the Engineering Mechanics Division (ASCE) 104(5) (1978) 1059-1079.
[9] Z.P. Bažant, J.C. Chern, W. Thonguthai, Finite element program for moisture and heat transfer in heated concrete, Nuclear Engineering & Design 68(1) (1980) 61-70.
[10] Z.P. Bažant, W. Thonguthai, Pore pressure in heated concrete walls - theoretical prediction, Magazine of Concrete Research 31(107) (1979) 67-76.
[11] B. Bary, A polydispersed particle system representation of the porosity for non-saturated cementitious materials, Cement and Concrete Research 36(11) (2006) 2061.
[12] L.J. Klinkenberg, The permeability of porous media to liquid and gases, American Petroleum Institute, Drilling and Production Practice (1941) 200-214.
[13] CEN, Hygrothermal performance of building materials and products - Determination of hygroscopic sorption properties, European Committe for Standardization (CEN), European Standard EN ISO 12571 (2000) 17p.
[14] OIML, The scale of relative humidity of air certified against saturated salt solutions, International Organization of Legal Metrology (OIML), Recommendation R 121 (1996) 12p.
[15] V. Baroghel-Bouny, Water vapour sorption experiments on hardened cementitious materials: Part I. Essential tool for analysis of hygral behaviour and its relation to pore structure, Cement and Concrete Research 37(3) (2007) 414-437.
[16] Xu Aimin, Water desorption isotherms of cement mortar with fly ash, Nordic Concrete Research 8 (1989) 9-23.
[17] R.M. Espinosa, L. Franke, Influence of the age and drying process on pore structure and sorption isotherms of hardened cement paste, Cement and Concrete Research 36(10) (2006) 1969-1984.
[18] V. Baroghel-Bouny, B. Perrin, L. Chemloul, Détermination expérimentale des propriétés hydriques des pâtes de ciment durcies - Mise en évidence des phénomènes d'hystérésis (in french), Materials and Structures 30(6) (1997) 304-348.
[19] F. Radjy, C.W. Richards, Effect of curing and heat treatment history on the dynamic mechanical response and the pore structure of hardened cement paste, Cement and Concrete Research 3(1) (1973) 7-21.
[20] V. Baroghel-Bouny, M. Mainguy, T. Lassabatere, O. Coussy, Characterization and identification of equilibrium and transfer moisture properties for ordinary and high-performance cementitious materials, Cement and Concrete Research 29(8) (1999) 1225-1238.
[21] S. Tada, K. Watanabe, Dynamic determination of sorption isotherm of cement based materials, Cement and Concrete Research 35(12) (2005) 2271-2277.
[22] R.S. Mikhail, G.A. Oweimreen, Surface area and pore structure of compressed low-porosity cement pastes, Cement and Concrete Research 3(5) (1973) 561-573.
[23] CEN, Testing hardened concrete, part I: shape, dimensions and other requirements for test specimens and moulds, European Committee for Standardization, European Standard EN 12390-1 (2001) 10p.
[24] J.J. Beaudouin, B.T. Tamtsia, Effect of drying methods on microstructural changes in hardened cement paste: an A.C. impedance spectroscopy evaluation, Journal of Advanced Concrete Technology 2(1) (2004) 113-120.
[25] C. Gallé, Effect of drying on cement-based materials pore structure as identified by mercury intrusion porosimetry. A comparative study between oven-, vacuum-, and freeze-drying, Cement and Concrete Research 31(10) (2001) 1467-1477.

[26] G.G. Litvan, Variability of the nitrogen surface area of hydrated cement paste, Cement and Concrete Research 6(1) (1976) 139-144.
[27] J.J. Beaudouin, J. Marchand, Pore structure, in: V.S. Ramachandran and J.J. Beaudouin (Eds), Handbook of analytic techniques in concrete science and technology, Noyes Publications, Park Ridge, USA, 2001, 528-628.
[28] M.C. Garci Juenger, H.M. Jennings, The use of nitrogen adsorption to assess the microstructure of cement paste, Cement and Concrete Research 31(6) (2001) 883-892.
[29] A. Korpa, R. Trettin, The influence of different drying methods on cement paste microstructures as reflected by gas adsorption: comparison between freeze-drying, D-drying, P-drying and oven-drying, Cement and Concrete Research 36(4) (2006) 634-649.
[30] J. Adolphs, A. Schreiber, Microstructural characterization of Ultra-High Performance Concrete, in: M. Schmidt, E. Fehling and C. Geisenhanslüke (Eds), Proceedings of the International Symposium on Ultra-High Performance Concrete, Kassel (Germany), Kassel University, 2004, 265-271.
[31] I. Pane, W. Hansen, Surface characteriation of blended cements by H_2O and N_2 sorption isotherms, in: J. Weiss, K. Kovler, J. Marchand and S. Mindess (Eds), Proceedings of the the 1st International Symposium on Advances in Concrete through Science and Engineering, Chicago, USA, RILEM PRO048, 2004.
[32] B.P. Hughes, I.R.G. Lowe, J. Walker, The diffusion of water in concrete at temperatures between 50 and 95℃, British Journal of Applied Physics 17(12) (1966) 1545-1452.
[33] N.L. Hancox, The role of moisture diffusion in the drying of cement paste under the influence of temperature gradients, Journal of Physics D: Applied Physics 1(12) (1968) 1769-1777.
[34] R. Černy, J. Drchalová, P. Rovnaníková, The effects of thermal load and frost cycles on the water transport in two high-performance concretes, Cement and Concrete Research 31(8) (2001) 1129-1140.
[35] S.F. Wong, T.H. Wee, S. Swaddiwudhipong, S.L. Lee, Study of water movement in concrete, Magazine of Concrete Research 53(3) (2001) 205-220.
[36] T.C. Powers, H.M. Mann, L.E. Copeland, The flow of water in hardened Portland cement paste, Portland Cement Association Bulletin 106 (1959) 18p.
[37] R.B. Anderson, Modifications of the Brunauer, Emmett and Teller equation, Journal of the American Chemical Society 68(4) (1946) 686-691.
[38] C. van der Berg, Vapour sorption equilibria and other water-starch interactions: a physico-chemical approach, Ph-D thesis, Agricultural University of Wageningen, The Netherlands, 1981, 186p.
[39] S. Brunauer, J. Skalny, E.E. Bodor, Adsorption on non porous solids, Journal of Colloid and Interface Science 30(4) (1969) 546-552.
[40] P.-N.T. Johnson, J.G. Brennan, Moisture sorption isotherm characteristics of plantain (*Musa*, AAB), Journal of Food Engineering 44(2) (2000) 79-84.
[41] C.P. McLaughlin, T.R.A. Magee, The determination of sorption isotherm and the isosteric heats of sorption for potatoes, Journal of Food Engineering 35(3) (1998) 267-280.
[42] A. Jonquières, A. Fane, Modified BET models for modeling water vapor sorption in hydrophilic glassy polymers and systems deviating strongly from ideality, Journal of Applied Polymer Science 67(8) (1998) 1415-1430.
[43] L.-T. Lim, I.J. Britt, M.A. Tung, Sorption and transport properties of water in Nylon 6,6 Film, Journal of Applied Polymer Science 71(2) (1999) 197-206.
[44] Y. Xi, Z.P. Bažant, H.M. Jennings, Moisture diffusion in cementitious materials - Adsorption isotherms, Advanced Cement Based Materials 1(6) (1994) 248-257.
[45] S. Bonnet, B. Perrin, Influence de la présence des ions chlorures sur les propriétés à l'équilibre de différents mortiers (chloride influence on equilibrium properties of mortars), Materials and Structures 32(7) (1999) 492-499.

[46] A. Xu, Water desorption isotherms of cement mortar with fly ash, Nordic Concrete Research 8 (1989) 9-23.
[47] S. Brunauer, P.H. Emmett, E. Teller, Adsorption of gases in multimolecular layers, Journal of the American Chemical Society 60(2) (1938) 309-319.
[48] IUPAC, Commission on Colloid and Surface Chemistry: Reporting physisorption data for gas/solid systems with special reference to the determination of surface area and porosity (Recommendations 1984), Pure and Applied Chemistry 57(4) (1985) 603-619.
[49] J.B. Condon, Surface area and porosity determinations by physisorption - Measurements & theory, Elsevier, 2006, 274p.
[50] S.J. Gregg, K.S.W. Sing, Adsorption, surface area and porosity, Academic Press, London, United Kingdom, 1982, 303p.
[51] V. Baroghel-Bouny, Caractérisation des pâtes de ciment et des bétons: Méthodes, analyse, interprétations (in french), Presses du Laboratoire Central des Ponts et Chaussées, Paris, France, 1994, 468p.
[52] I. Odler, The BET-specific surface area of hydrated Portland cement and related materials, Cement and Concrete Research 33(12) (2003) 2049-2056.
[53] J.J. Thomas, H.M. Jennings, A.J. Allen, The surface area of hardened cement paste as measured by various techniques, Concrete Science and Engineering 1(1) (1999) 45-64.
[54] I. Odler, J. Hagymassy, M. Yudenfreund, K.M. Hanna, S. Brunauer, Pore structure analysis by water vapor adsorption. IV. Analysis of hydrated portland cement pastes of low porosity, Journal of Colloid and Interface Science 38(1) (1972) 265-276.
[55] J. Skalny, I. Odler, Pore structure of calcium silicate hydrates, Cement and Concrete Research 2(4) (1972) 387-400.
[56] J. Hagymassy, I. Odler, M. Yudenfreund, J. Skalny, S. Brunauer, Pore structure analysis by water vapor adsorption. III. Analysis of hydrated calcium silicates and portland cements, Journal of Colloid and Interface Science 38(1) (1972) 20-34.
[57] R.S. Mikhail, S.A. Abo-El-Enein, Studies on water and nitrogen adsorption on hardened cement pastes I - Development of surface in low porosity pastes, Cement and Concrete Research 2(4) (1972) 401-414.
[58] W.H. Bray, E.J. Sellevold, Water sorption properties of hardened cement paste cured or stored at elevated temperatures, Cement and Concrete Research 3(6) (1973) 723-728.
[59] E.J. Sellevold, Mercury porosimetry of hardened cement paste cured or stored at 97℃, Cement and Concrete Research 4(3) (1974) 399-404.
[60] T.C. Powers, T.L. Brownyard, Studies of the physical properties of the hardened cement paste, Portland Cement Association Bulletin 22 (1948) 356p.
[61] P.C. Carman, F.A. Raal, Role of capillary condensation in physical adsorption, Nature 167 (1951) 112-113.
[62] P.C. Carman, F.A. Raal, Physical adsorption of gases on porous solids I - Comparison between loose powders and porous plugs, Proceedings of the Royal Society of London - Series A, Mathematical and Physical Sciences 209(1096) (1951) 59-69.
[63] P.C. Carman, Physical adsorption of gases on porous solids II - Calculation of pore-size distribution, Proceedings of the Royal Society of London - Series A, Mathematical and Physical Sciences 209(1096) (1951) 69-81.
[64] R.G. Avery, J.D.F. Ramsay, The sorption of nitrogen in porous compacts of silica and zirconia powders, Journal of Colloids and Interface Science 42(3) (1973) 597-606.
[65] S.J. Gregg, J.F. Langford, Study of the effect of compaction on the surface area and porosity of six powders by measurements of nitrogen sorption isotherms, Journal of the Chemical Society - Faraday Transactions I 73 (1977) 747-759.
[66] S. Brunauer, The adsorption of gases and vapors - Volume I - Physical adsorption, Princeton University Press, 1945, 511p.

[67] D. Myers, Surfaces, interfaces and colloids - Principles and applications, John Wiley, New York, USA, 1999, 519p.
[68] J. Keller, R. Staudt, Gas adsorption equilibria - Experimental methods and adsorption isotherms, Springer Science, Boston, Massachussets, USA, 2005, 422p.
[69] A.A. Fomkin, Adsorption of gases, vapors and liquids by microporous adsorbents, Adsorption 11(3) (2005) 425-436.
[70] I.I. Salame, T.J. Bandosz, Experimental study of water adsorption on activated carbons, Langmuir 15(2) (1999) 587-593.
[71] I.I. Salame, T.J. Bandosz, Adsorption of water and methanol on micro- and mesoporous wood-based activated carbons, Langmuir 16(12) (2000) 5435-5440.
[72] D.D. Do, Adsorption analysis: equilibria and kinetics, Series on Chemical Engineering Vol. 2, Imperial College Press, London, United Kingdom, 1998, 913p.
[73] R.T. Yang, Adsorbents: fundamentals and applications, John Wiley and Sons, Hoboken, New Jersey, USA, 2003, 425p.
[74] M. Suzuki, Adsorption engineering, Elsevier Science, Amsterdam, The Netherlands, 1990, 270p.